Beamforming and Tracking Assessment with Passive Radar Experimental Data

Tri-Tan Van Cao*, Tuyet Vu*, Marion Byrne*, Nabaraj Dahal*, Paul E. Berry*, Ayobami B. Iji*, Daniel Gustainis*, Martin Ummenhofer** and Michael Kohler**
* Defence Science & Technology (DST) Group, Adelaide, Australia
** Fraunhofer Institute for High Frequency Physics and Radar Techniques (Fraunhofer FHR), Wachtberg, Germany

***Abstract*—Using experimental data captured with a passive radar linear array built by Defence Science and Technology (DST) Group, the performance of various beamforming algorithms (beamformers) for direction-of-arrival (DoA) estimation is comparatively assessed. Beamformers' DoA estimates are passed to a tracker which performs angle tracking, and the resulting track quality is examined based on the Optimal Sub-Pattern Assignment Metric for Multiple Tracks (OSPAMT). By matching the ground-truth tracks with the confirmed tracks, the OSPAMT takes into account both the locality error (how close the confirmed tracks are to the ground-truth tracks) and the cardinality error (the numbers of false tracks, track breaks and missed tracks). The best OSPAMT score is achieved by a newly-designed sparse solution beamformer derived from a compressive sensing principle and based on off-grid approaches.**

Keywords— Passive radar; array beamforming; tracking; OSPAMT; compressive sensing; sparse approximation; direction-of-arrival estimation.

I. INTRODUCTION

Target detection and tracking are two basic functions of a radar. In target tracking, target localization in direction-of-arrival (DoA) plays an important role. For a passive radar (PR) equipped with an array receiver, a DoA estimation procedure consists of a beamforming algorithm (beamformer) and a search over the radar field-of-view (FoV) to take advantage of a surveillance space which has been illuminated constantly by illuminators of opportunity [1,2].

There are two types of beamformers: (1) conventional delay-and-sum (DS) beamformers whose computation (such as beamformer weights) is independent of the observed signal and noise characteristics, and (2) adaptive beamformers whose computations depend on the characteristics of the received signals and noise (for instance, beamformer weights depending on the observed noise covariance matrix). There are situations where DS beamformers provide optimal performance despite their computational simplicity, whereas in other situations better performance can be achieved using an adaptive beamformer [3]. For passive radar applications, DS beamformers are known to be capable of real-time operation [1], while applications of adaptive beamformers such as Minimum Variance Distortionless Response (MVDR), Multiple Signal Classification (MUSIC), root-MUSIC (R-MUSIC), phase comparison monopulse, and Compressive Sensing (CS) beamformers have also been reported [4].

A popular approach to assessing a beamformer's performance is based on criteria such as DoA estimation precision (how well DoA measurements match DoA ground truth), beamformer resolution (the ability to resolve two closely spaced targets in DoA), maximum side-lobe level (the ability to reject unwanted sources), the assumption of known number of sources, scanning requirement and computational load [3]. However, this traditional assessment does not capture the consistency of the beamformer's performance over time, which is an important characteristic in determining the quality of target tracking.

There are two new contributions in this paper: (1) a different approach to beamformer performance assessment using the framework of multi-target tracking (MTT) quality assessment is adopted, which captures the consistency of performance over time of a beamformer while allowing the incorporation of the characteristics addressed by the traditional assessment; and (2) a new sparse solution beamformer based on CS principles is derived using off-grid approaches.

Since a beamformer's outputs are employed for target tracking, a comprehensive way to assess a beamformer's performance is to examine the resulting track quality. The beamformer evaluation can then be addressed in the MTT quality assessment framework, which involves the measurement of distance between the set of ground-truth tracks and the set of confirmed tracks. To this end, two types of distances (errors) between two sets of tracks are considered: the locality error and the cardinality error [5, 6]. Locality error is the Euclidean distance between the DoA tracks and the DoA ground truth. Cardinality error takes into account the number of confirmed tracks compared with the number of true tracks.

Both the locality and cardinality errors were originally incorporated into a metric called Optimal Sub-Pattern Assignment (OSPA) between two sets of vectors [7]. For target tracking assessment, a metric for sets of tracks is required. For this purpose, in [8], the OSPA metric was developed further as OSPA for tracks (OSPAT), in which the core idea is to add in a track label error in order to capture the data association performance; however OSPAT is not a metric [5]. The OSPA metric was then extended to OSPAMT (OSPA metric for multiple tracks), which does not require an ad-hoc distance between target labels while capturing key MTT features including missed tracks, false tracks, and track breaks [5, 6].

CS principles have been employed for DoA estimation [4, 9, 10]. In the CS literature, the Fast Sparse Functional Iteration Algorithm (FSFIA) has been developed as a general-purpose tool for solving the Basis Pursuit Denoising problem and has been used for a number of sparse signal estimation radar applications such as tomography and signal separation [10-12]. It solves the least squares minimisation problem of fitting a dense grid of potential scatterers to a measured set of signals, regularized by the l_1-norm. In this paper, FSFIA is applied to passive bistatic DoA estimation in

978-1-7281-6813-5/20/$31.00 ©2020 Crown

a sparse scene; its performance in the MTT assessment framework is experimentally demonstrated to be superior to other currently available state-of-the-art beamformers. We investigate off-grid approaches and propose a new beamformer in which the FSFIA operates on an adaptive DoA grid.

The paper is arranged as follows. The newly-proposed Sparse-Adaptive beamformer is presented in Section II, and the beamformer assessment procedure is described in Section III. A summary of other beamformers for performance comparison is also given in Section III. Calculation of the OSPAMT score is presented in Section IV, while description of the PR data and experimental results are presented in Sections V. Major findings are then discussed in Section VI.

II. Adaptive-Grid Sparse Solution Beamformer

The sparse solution beamformers with k iterations using a static grid and an adaptive grid, denoted as Sk-Static and Sk-Adap, respectively, are presented in this section.

The DoA parameter space θ of an N-element linear array is discretized into L spatial sampling points ($L > N$), each sample point (known as 'atom') being a potential signal source, and the set of all those atoms is referred to as a dictionary. Assume that there are L such potential signal sources of complex amplitude a_l and corresponding DoA θ_l ($l = 1, \dots, L$), which are represented by the column vector $\boldsymbol{a}$ (of length L), and that the matrix $\boldsymbol{S}$ (of size $N \times L$) has columns which are the steering vectors of the atoms in the dictionary (so $\boldsymbol{S}$ represents a discretized array manifold). The $N \times 1$ signal vector $\boldsymbol{b}$ observed at the N-element array is:

$$\boldsymbol{b} = \boldsymbol{S}\boldsymbol{a} + \boldsymbol{n} \tag{1}$$

where $\boldsymbol{n}$ is the noise vector. The DoA estimation problem is expressed as a regularised l_1-optimization problem as:

$$\min_{\boldsymbol{a}} \left\{ ||\boldsymbol{a}||_1 + \tfrac{1}{2}\mu ||\boldsymbol{S}\boldsymbol{a} - \boldsymbol{b}||_2^2 \right\} \tag{2}$$

which means, find $\boldsymbol{a}$ which minimises the error between the observed signal and the model in the least-squares sense while keeping the number of non-vanishing coefficients of $\boldsymbol{a}$ to a minimum. Using a Lagrange multiplier for the single constraint, the following nonlinear equations are satisfied at the stationary point w.r.t. the complex vector $\boldsymbol{a}$:

$$[\boldsymbol{I}_L + \mu \boldsymbol{\Lambda}(\boldsymbol{a}) \boldsymbol{S}^H \boldsymbol{S}] \boldsymbol{a} = \mu \boldsymbol{\Lambda}(\boldsymbol{a}) \boldsymbol{S}^H \boldsymbol{b} \tag{3}$$

where $\boldsymbol{I}_L$ is an $L \times L$ identity matrix and $\boldsymbol{\Lambda}(\boldsymbol{a})$ is a diagonal matrix whose diagonal elements are the moduli $|a_l|$, $l = 1, \dots, L$. Applying functional iteration instead of Newton-Raphson iteration, a solution to this nonlinear equation can be obtained without needing to compute the Jacobian. At the n^{th} iteration, the solution $\boldsymbol{a_{n+1}}$ to the following $L \times L$ linear system is required:

$$[\boldsymbol{I}_L + \mu \boldsymbol{\Lambda}(\boldsymbol{a_n}) \boldsymbol{S}^H \boldsymbol{S}] \boldsymbol{a_{n+1}} = \mu \boldsymbol{\Lambda}(\boldsymbol{a_n}) \boldsymbol{S}^H \boldsymbol{b} \tag{4}$$

The Woodbury matrix identity can then be used to show:

$$[\boldsymbol{\Lambda}^{-1} + \mu \boldsymbol{S}^H \boldsymbol{S}]^{-1} \equiv \boldsymbol{\Lambda} - \boldsymbol{\Lambda}\boldsymbol{S}^H [\mu^{-1}\boldsymbol{I} + \boldsymbol{S}\boldsymbol{\Lambda}\boldsymbol{S}^H]^{-1} \boldsymbol{S}\boldsymbol{\Lambda} \tag{5}$$

so that only solutions to a smaller $N \times N$ linear system are required (in this application, $N = 7$ whereas $L = 241$).

One of the drawbacks of using a dictionary with a static grid of atoms is to limit DoA angular resolution. The predefined static grid incurs energy spread around neighboring atoms due to grid mismatch resulting in poor resolution. One of the solutions to this problem would be to increase the number of atoms in the dictionary by reducing the grid interval step. However, this would result in higher mutual correlation between the atoms leading to poor DoA estimation. This is referred to as the off-grid problem. A better approach to solve this problem is to allow the grid to dynamically adapt in parameter space $\boldsymbol{\theta}$ and solve the optimization problem in equation (2) to jointly estimate the sparse vector $\boldsymbol{a}$, and grid parameter vector $\boldsymbol{\theta}$ of matrix S.

In the proposed adaptive-grid approach, FSFIA (4) is used for the non-linear least square minimization w.r.t. $\boldsymbol{a}$, whereas Gauss-Newton iteration (6) is used to solve the minimization w.r.t. $\boldsymbol{\theta}$ so as to successively refine the sparse vector $\boldsymbol{a}$ and the grid position $\boldsymbol{\theta}$ in each iteration:

$$\boldsymbol{\theta}^{n+1} = \boldsymbol{\theta}^n - J(\boldsymbol{\theta}^n)^{\dagger} f(\boldsymbol{\theta}^n) \tag{6}$$

where the Jacobian

$$J(\boldsymbol{\theta}) = \frac{\partial f}{\partial \theta} \tag{7}$$

with the Moore-Penrose pseudo-inverse (or Generalized inverse) of the Jacobian as:

$$J^{\dagger} \equiv (J^H J)^{-1} J^H \tag{8}$$

The adaptive-grid FSFIA algorithm starts with the initialization from k iterations of the static FSFIA algorithm. Then after, n atoms with the highest amplitude of $\boldsymbol{a}$ are chosen for the grid position update. The detailed algorithm is summarised in Table I.

TABLE I: ADAPTIVE-GRID FSFIA ALGORITHM

---

input:
- -The output vector $\boldsymbol{a}$ from Sk-static FSFIA.
- -The initial grid parameter $\boldsymbol{\theta}$.

begin iteration
- -Choose n atoms with highest amplitudes from $\boldsymbol{a}$.
- -Update position for n atoms in $\boldsymbol{\theta}$ using G-N equation (6).
- -Update dictionary $\boldsymbol{S}$ with the new positions of n atoms.
- -Refine $\boldsymbol{a}$ using updated $\boldsymbol{S}$ using FSFIA equation (4).

end iteration

iteration stopping criteria:
- -Stop when the updated atom positons cross the neighboring atom positions.

output:
- -Sparse vector $\boldsymbol{a}$.
- -Updated grid parameter $\boldsymbol{\theta}$.

The updated space parameter $\boldsymbol{\theta}$ obtained on initializing the adaptive grid FSFIA algorithm with k iterations of static FSFIA is referred to as the Sk-Adap FSFIA output.

III. Beamformer Assessment Methodology

For each beamformer under consideration, a target's DoA is estimated over time using experimental data collected by the N-channel linear array of a PR system. DoA estimates are then used to form target tracks which are compared with the ground truth tracks to calculate the beamformer's OSPAMT score. The OSPAMT scores are then used to rank a beamformer's performance.

A target's DoA is estimated as follows. The radar FoV is divided into a grid of L=241 points, covering an angular sector of [-60°, +60°] in steps of Δ=0.5°. The steered response of the array (which shows how the array output varies with assumed propagation direction specified by the steering vector) is computed at each grid point, producing the beamformer DoA output. From this DoA profile, the largest local peak is selected and the corresponding angle θ is the DoA measurement.

The following beamformers are considered for comparison with the sparse beamformers: from the DS group: Uniform, Chebyshev and amplitude monopulse; from

the adaptive group: MVDR, MUSIC, R-MUSIC, and ESPRIT (Estimation of Signal Parameters via Rotational Invariance Techniques).

For DS beamformers, each receive element of the array is phase-shifted by an appropriate amount (determined by the steering vector), multiplied by set of amplitude weights known as the array taper vector, and then summed together to give the array output [3]. The DS beamformer is then named after the method used to design the taper vector. Two DS beamformers are considered, namely: Uniform beamformer (the array is not tapered); and Chebyshev beamformer (the array is tapered using a Chebyshev window). The DoA is determined by the maximum response from the search of the DoA profile.

For monopulse beamformers, firstly the steered response using the Chebyshev beamformer is computed in a coarse grid covering the same angular sector [-60º, +60º]. In this paper, 61 grid points with a step of Δ=2º are used. The local peak selection gives an estimate of the DoA θ within the coarse uncertainty interval [θ-Δ, θ+Δ]. Secondly, the whereabouts of the target in the interval [θ-Δ, θ+Δ] is refined using amplitude monopulse (A-mnp) [13, 14].

For the MVDR beamformer, the output power at DoA θ is:

$$P(\theta) = \frac{1}{\boldsymbol{s}^H(\theta)\widehat{\mathbf{R}}^{-1}\boldsymbol{s}(\theta)} \tag{9}$$

where $\boldsymbol{s}(\theta)$ is the steering vector and $\widehat{\mathbf{R}}$ is the covariance matrix estimate which can be obtained using an autocorrelation of the data and Toeplitz matrix approximation [3,4].

For the MUSIC beamformer, eigenvalue decomposition is performed on the covariance matrix estimate $\widehat{\mathbf{R}}$, giving $\widehat{\mathbf{R}}\mathbf{V} = \mathbf{V}\mathbf{L}$, where $\mathbf{L}$ is a diagonal matrix formed by N eigenvalues $l_1, l_2, \ldots, l_N$ with $l_1 \geq l_2 \geq \ldots \geq l_N$, and $\mathbf{V} = [\mathbf{v}_1, \mathbf{v}_2, \ldots, \mathbf{v}_N]$ in which $\mathbf{v}_k$ is the (column) eigenvector associated with eigenvalue l_k. Assuming that the number of signal sources n is known (or can be estimated), then the set of noise (signal-free) eigenvectors is $\mathbf{V}_n = [\mathbf{v}_{n+1}, \mathbf{v}_{n+2}, \ldots, \mathbf{v}_N]$. The output power of the MUSIC beamformer at DoA θ is then [3]:

$$P(\theta) = \frac{1}{\boldsymbol{s}^H(\theta)\boldsymbol{V_n}\boldsymbol{V}_n^H\boldsymbol{s}(\theta)} \tag{10}$$

For R-MUSIC [4,15], a polynomial is formed from the diagonals of $\mathbf{V}_n\mathbf{V}_n^H$. For the single target assumption, the root z_0 of this polynomial which is closest to the unit circle determines the DoA. In case of multiple targets, several roots close to the unit circle are selected.

For ESPRIT, the antenna is partitioned into two overlapping sub-arrays, each with N-1 antenna elements: one comprises antenna elements from the 1st to the 2nd-last (i.e. 1, ..., N-1) and the other one comprises antenna elements from the 2nd to the last (i.e. 2, ..., N). The signal portions of those two sub-arrays, denoted as S_1 and S_2, are related as $S_1 = S_2\Phi$, in which Φ is a diagonal matrix with elements corresponding to the inter-subarray propagation delays [3]. Φ is found through the eigen-analysis of the covariance matrix estimate and then is used for DoA estimation. Details of ESPRIT implementation can be found in [16].

IV. TRACKING ALGORITHM AND OSPAMT

A. Tracking Algorithm

A Kalman Filter [17] is used to form track state estimates of azimuth and azimuth-rate from the DoA measurements. A nearly-constant azimuth-rate motion model is assumed, and the algorithm uses the true variance of the set of measurements for a given beamformer as the modelled measurement variance. The tracking algorithm performs multiple target tracking to account for clutter and missed detections in the beamformer outputs. Measurements are associated with tracks using a global nearest-neighbour approach, measured by the Mahalanobis distance and applying an ellipsoidal gate which sets a one-dimensional assignment probability of 90% [18, section 6.4]. Tracks are initiated using a one-point, zero azimuth rate initiation scheme with zero mean noise. A track is confirmed when the ratio of missed detections in the track's life falls below a given threshold. If a track has more than 6 consecutive missed detections, it is terminated.

B. OSPAMT

The implementation of the OSPAMT formula for the case of a single true track/multiple confirmed tracks is summarized here. See [5, 6] for the general case of multiple true tracks/multiple confirmed tracks.

Let $\tau = \{x(1), \ldots, x(K)\}$ be the state vector of the true track, where $x(n)$ is the true target DoA at time index n (n=1,…,K). This true target exists for all time in each data set. Assume that there are M confirmed tracks $\tau_1, \ldots, \tau_M$. Let $\tau_m = \{x_m(t_{m,1}), \ldots, x_m(t_{m,K_m})\}$ be the state vector of the confirmed track τ_m (m = 1,…,M), where $x_m(t_{m,k})$ is the DoA value of track τ_m at time index $1 \leq t_{m,k} \leq K$, (k =1,… K_m). The OSPAMT score is calculated as follows. Select two constants: Δ (the track break penalty which is applied over the duration of an extra associated track) and c (the cardinality error penalty). For this application, c=80 and Δ=0.5.

- Step 1: designate associated and false tracks
  a) For each confirmed track τ_m, m=1,…,M, at each time n, calculate the distance $d_m(n)$ as

$$d_m(n) = \begin{cases} \bar{d}_m(n), \text{ if } \bar{d}_m(n) < c \text{ and } t_{m,1} \leq n \leq t_{m,K_m} \\ c, \text{ otherwise} \end{cases}$$

where $\bar{d}_m(n) = |x_m(n) - x(n)|, \; t_{m,1} \leq n \leq t_{m,K_m}$ (11)

  b) Then find the average distance between track τ_m and the true track τ, $d_{m,ave} = \left(\frac{1}{K}\right)\sum_{n=1}^{K} d_m(n)$
  c) Recursively, the undesignated track τ_m with the smallest $d_{m,ave}$ less than c and with at least one time step $t_{m,k}$ not included in an already associated track is designated an 'associated track'. All tracks not associated at the end of this recursion are designated as 'false tracks'.
- Step 2: for n=1 to K
  a) Count the number of the associated tracks $T_a(n)$ and the number of false tracks $T_f(n)$ at this time according to Step 1;
  b) Count the number of missed tracks $T_m(n)$. One missed track is counted at time index n if there is no associated track at this time index; otherwise, there are no missed tracks;
  c) Calculate $T_{track}(n)$ which is the maximum of two numbers: the number of true tracks (1 in this data)

and the number of confirmed tracks at time index n;

d) Calculate, at time index n, the absolute distance(s) between the associated track (if more than one track associated with the true track, the one with the smallest $d_{m,ave}$ is chosen) and the true track at this time;

e) Calculate $d_{sum}(n)$, the summation of all the absolute distances in step 2(d) at time index n.

f) The locality error is then:

$$d_{Loc}(n) = \frac{d_{sum}(n)+\Delta \max(T_a(n)-1,0)}{T_{track}(n)} \quad (12)$$

g) The cardinality error is then:

$$d_{Car}(n) = \frac{1}{T_{track}(n)}\left(T_f(n) + T_m(n)\right)c \quad (13)$$

- Step 3: average over the scenario

a) Let $\bar{d}_{Loc} = (1/T_{track}) \sum_{n=1}^{K} T_{track}(n)\, d_{Loc}(n)$ and $\bar{d}_{Car} = (1/T_{track}) \sum_{n=1}^{K} T_{track}(n) d_{car}(n)$, where $T_{track} = \sum_{n=1}^{K} T_{track}(n)$;

b) The total OSPAMT score is then:

$$\bar{d} = \bar{d}_{Loc} + \bar{d}_{Car} \quad (14)$$

V. Experimental Data and Results

Experimental data was obtained from a PR system built by Defence Science and Technology (DST) Group, which consists of a uniform linear array (ULA) having seven vertically polarized, low gain folded dipole antenna elements that were designed to operate in the Ultra High Frequency (UHF) band between 520MHz and 620MHz. The antenna's inter-element spacing is 263mm. The radar FoV covers an azimuth sector between -60° and +60° with respect to the array's boresight. A photo of the ULA is shown in Figure 1.

To mitigate direct signal interference from the illuminators of opportunity, the antenna array is fitted with a reflective backplane positioned at a distance of 210mm from the folded antenna to suppress the effect of back-lobe. The ULA achieves a gain of 15.7dBi and an azimuth beam-width of 15 degrees. The array was mounted on a tilt device which was tilted 82 degrees upwards with respect to the horizontal plane at the time of data capture.

The PR system was deployed at approximately 20 km north of Adelaide central business district, with its antenna boresight pointing to 295^{O} relative to true North. The primary goal of the experiment was the demonstration of a PR's ability to perform accurate target angle measurements in the azimuth plane for target bearing estimation. Targets of opportunity were approximately 4 to 30 km from the receiver, consisting of air traffic near Parafield Airport and aircraft departing and approaching Adelaide Airport (comprising mostly of twin engine narrow body aircraft down to single engine turboprops). Ground-truth data of their state vectors was collected with an ADS-B (Automatic Dependent Surveillance-Broadcast) receiver. The system works in a bistatic configuration and uses a DVB-T (Digital Video Broadcast -Terrestrial) opportunistic transmitter which is 30 km from the receiver and 164^{O} from true North.

Figure.1 The experimental passive radar uniform linear array antenna.

The above-mentioned beamformers were applied to seventeen target data files collected by the ULA described in Section V. For a given data set, formation of the Direction Finding (DF) map was performed using the Uniform beamformer, followed by a constant false rate alarm (CFAR) detection [2]. Detections whose range and Doppler (RD) in the DF-map matched with the RD ground truth of a real target were then extracted and passed to the beamformers for beamforming assessment. In the set of those RD matched detections, there may be false alarms as well as missed detections compared to the true track of the real target.

Figure 2 shows DoA tracks over time of beamformers Uniform, R-MUSIC and S05-Static versus the DoA ground-truth for File 2. In terms of locality error, the beamformers are very similar to each other since all the confirmed tracks are close together. In terms of cardinality error, there are track breaks for beamformers Uniform and R-MUSIC around time instant 38s; only the S05-Adap has no track breaks. DoA tracks of beamformers S02-Adap and MVDR for File 15 are shown in Figure 3. For this slightly manoeuvring DOA scenario, while the S02-Adap does not have any track break (Figure 3, top), the MVDR has a track break around time instant 14s (Figure 3, bottom). The tracks of those two beamformers are comparatively close to the ground truth. Locality and cardinality errors of the amplitude monopulse beamformer for File 2 are presented in Figure 4. The locality errors within the first-half time interval [0, 20s] are smaller than those within the second-half time interval [40s, 67s] as shown in Figure 4 (bottom). This is consistent with the observation in Figure 4 (top), in that the DoA measurements within the second-half time interval are also closer to the DoA ground truth. The large cardinality errors at time 38s, 45s and 50s (Figure 4, bottom) are due to the track breaks and missed tracks at those time instants (there is only one true target track in this case).

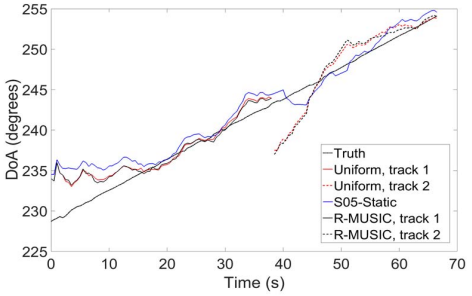

Figure 2. DoA tracks of beamformers Uniform, R-MUSIC and S05-Static for File 2.

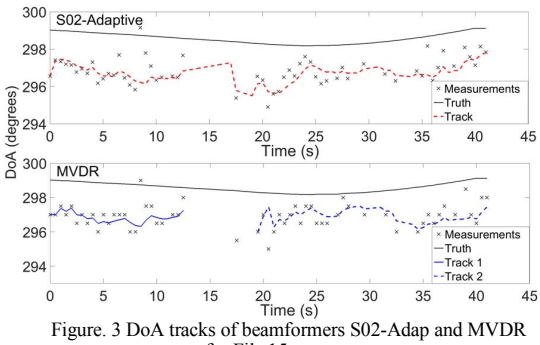

Figure. 3 DoA tracks of beamformers S02-Adap and MVDR for File 15.

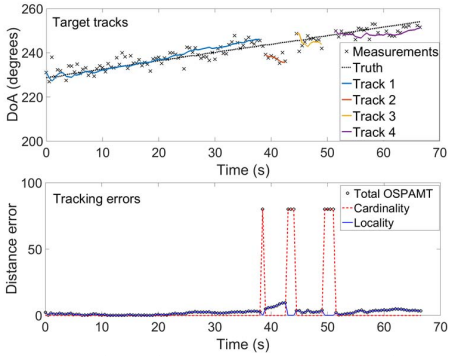

Figure 4. Locality and cardinality errors of monopulse, File 2.

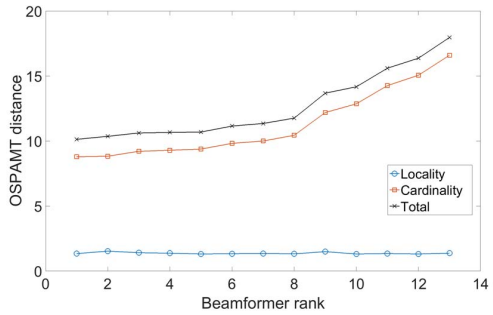

Figure 5. Average OSPAMT distances for all beamformers.

Ranking of all beamformers based on their OSPAMT scores (smaller is better) averaged over seventeen target data files are summarised in Table II. In this table: the average of $\bar{d}$, $\bar{d}_{Loc}$, and $\bar{d}_{Car}$ (equation (14)) are denoted as 'Total error', 'L-error' and 'C-error', respectively; for more detail regarding the cardinality error, the averages of the number of assigned tracks and the number of false tracks (found in Section IV.B, Step 2a) are denoted as 'D_a' (1 is best, greater than 1 means track breaks) and 'D_f' (0 is best), respectively; $\bar{P}_m = 100\left(\sum_{j=1}^{10} P_j/10\right)$, where P_j is defined as the ratio between the total time for which there are missed tracks and the duration of the data file for each file j (j = 1,…,17); the column 'Time' presents the time for computing one DoA profile. This time is measured using the Matlab 'tic-toc' time-lapse function, averaged over seventeen data sets, and then normalized to the averaged time-lapse of MVDR (the tic-toc time by itself is computer-dependent).

TABLE II. RANKING OF AVERAGE OSPAMT SCORES OVER 17 DATA SETS FROM BEST (TOP) TO WORST (BOTTOM)

Name	Beamformer performance						
	Total error	***L-error***	***C-error***	D_f	D_a	$\bar{P}_m$, %	***Time***
S02-Adap	10.13	1.34	8.79	0	1.22	10.59	6.98
S01-Static	10.36	1.53	8.83	0	1.33	11.03	0.30
S05-Adap	10.62	1.41	9.21	0	1.28	11.11	8.24
ESPRIT	10.66	1.37	9.29	0	1.39	8.35	0.28
MUSIC	10.69	1.31	9.38	0	1.22	11.34	0.36
R-MUSIC	11.15	1.33	9.82	0.06	1.22	10.73	0.51
Uniform	11.35	1.35	10.00	0	1.22	12.51	0.06
S05-Static	11.76	1.32	10.44	0.17	1.22	10.26	0.70
MVDR	13.68	1.49	12.19	0	1.33	15.01	1.00
S10-Static	14.17	1.31	12.86	0.17	1.39	13.54	1.32
Chebyshev	15.60	1.34	14.26	0.06	1.33	15.63	0.08
S50-Static	16.37	1.31	15.06	0.11	1.28	17.61	6.68
A-mnp	17.97	1.37	16.60	0.11	1.61	16.82	0.17

The S02-Adap has the best OSPAMT score, with the smallest C-error (its numbers of track breaks and false tracks are smallest, while its missed track percentage is third to smallest). However, the locality error of S02-Adap is larger than that of MUSIC which is the smallest in the

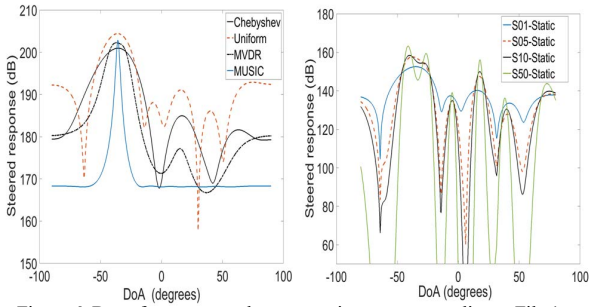

Figure 6. Beamformer steered responses in antenna coordinate, File 1.

ranking list. The simple Uniform beamformer performs better than the adaptive MVDR. As evident in Figure 5, there is a small difference between the locality errors of the top ranked and the bottom ranked beamformers. It is the cardinality errors that degrade their performance. The steered responses of the beamformers are shown in Figure 6. From Figure 6 left, MUSIC has the smallest 3-dB beamwidth while that of the Chebyshev is the broadest. In this application, such a large beamwidth does not cause any DoA estimation degradation since there is only one target within each target scenario. If there are multiple closely-spaced targets in DoA, the advantage of beamformers with narrow beamwidths may become apparent. The steered responses of the static-grid sparse beamformers are shown in Figure 6, right. In general, more iterations give finer 3-dB beamwidths.

VI. DISCUSSION

A. Sparse Beamformers: Static-Grid vs Adaptive-Grid

From Table II, the adaptive-grid beamformer has a smaller average cardinality error compared to the static-grid beamformer. This means that the consistency of the adaptive-grid's DoA estimates over time is improved compared to that of the static-grid. However, the use of adaptive grid does not show an improvement in terms of locality error (the L-error of S05-Adap is larger than that of the S05-static).

B. Sparse Beamformers: Effect of Iterations

In the sparse-static group, an increased number of iterations generally gives smaller average locality error (the tracks are closer to the true tracks); but it does not mean that the consistency of the measurements over time is improved. In Table II, although the S50-Static has the smallest L-error,

its C-error is larger than those of the S10-Static and S05-Static.

C. Traditional Beamformer Assessment Criteria vs OSPAMT

OSPAMT scores are computed by mapping the set of confirmed tracks to the set of true tracks, and then calculating two types of distances between those two sets of tracks: the locality error and the cardinality error. The locality error captures the precision criteria in the traditional assessment. The cardinality error captures the ability of the beamformer in rejecting unwanted interferences coming from other directions as well as the ability of the beamformer to distinguish two closely spaced targets in DoA. Those types of interferences lead to outliers in the DoA estimates which may cause track breaks, false tracks and missed tracks. In short, beamformer assessment based on MTT and OSPAMT score captures the consistency of performance over time of a beamformer while allowing the incorporation of all the beamformer's assessment criteria addressed by the traditional assessment (except the beamformer's computational load).

Overall, it is evident that a beamformer with a better OSPAMT score has less track breaks, less false tracks and a smaller percentage of missed tracks, although its track is not necessarily closer to the true track since the L-errors of all beamfomers are very similar. From a practical point-of-view, those improved characteristics agree well with the fact that track breaks are problematic since the radar has to go through the search procedure again, while false tracks cause confusion to the radar operator, and missed tracks mean that the target enters the radar FoV for a long time without being tracked. As such, it is reasonable that those problematic errors should be heavily penalized in practice.

D. Real-Time Implementation

It is well-known that the non-adaptive DS beamformers are real-time capable (see [1], for instance). Any beamformer which has a normalized tic-toc smaller than those of the DS beamformers are potentially real-time capable. From Table II, the best S02-Adap and second-best S01-Static are approximately 100 times and 5 times, respectively, slower than the Uniform. As such, S01-Static (with only 1 iteration) is a stronger candidate for real-time implementation.

VII. Conclusion

A new beamforming technique, namely the adaptive-grid FSFIA based on compressive sensing principles, was derived and tested on experimental data collected by a passive ULA built by DST Group. The adaptive-grid FSFIA achieves the best performance compared with other currently available non-adaptive beamformers and state-of-the-art adaptive beamformers. Beamformers' performance assessment was performed in the MTT framework based on OSPAMT scores which allows the incorporation of the assessment criteria addressed by the traditional beamforming assessment approach while capturing the consistency in performance over time of a beamformer, being an important characteristic which has not been considered in the traditional beamformer evaluation. Such an alternative to the traditional beamformer evaluation is application-dependent and requires that experimental data is available for target tracking, which is the case for a PR system.

Acknowledgment

The support of the DST's Passive Radar Team is gratefully acknowledged. The ESPRIT code was provided thanks to Dr. Mayank Kaushik. The quality of the paper was enhanced thanks to the input of Prof. Daniel W. O'Hagan, Mr. Robert Young and Dr. Deane Prescott.

References

[1] G. Bournaka, J. Heckenbach, A. Baruzzi, D. Cristallini, and H. Kuschel Bournaka, "A Two Stage Beamforming Approach for Low Complexity CFAR Detection and Localization for Passive Radar", 2016 IEEE Radar Conference, Philadelphia, USA.

[2] T.V. Cao, "Sequential detection for Passive Radar, Part 1: the AC DFmap detector", 2018 IEEE Radar Conference, Brisbane.

[3] D.H. Johnson and D.E. Dudgeon, Array Signal Processing: Concepts and Techniques, Prentice Hall, Englewood Cliffs, 1993.

[4] M. Ummenhofer, M. Kohler, J. Schell, and D.W. O'Hagan, "Direction of Arrival Estimation Techniques for Passive Radar Based 3D Target Localization", 2019 Radar Conference, Boston, USA.

[5] T. Vu and R. Evans, "A New Performance Metric for Multiple Target Tracking Based on Optimal Subpattern Assignment", 17th International Conference on Information Fusion (FUSION), 2014, Salamanca, Spain.

[6] T. Vu and R. Evans, "Optimal Subpattern Assignment Metric for Multiple Tracks (OSPAMT Metric)," arXiv e-prints, p. arXiv:1808.02242, Aug 2018.

[7] D. Schuhmacher, B.-T. Vo, and B.-N. Vo, "A consistent metric for performance evaluation of multi-object filters," IEEE Trans. Signal Processing, vol. 56, no. 8, pp. 3447–3457, Aug. 2008.

[8] B. Ristic, B.-N. Vo, D. Clark, and B.-T. Vo, "A metric for performance evaluation of multi-target tracking algorithms," IEEE Transactions on Signal Processing, vol. 59, no. 7, p. 3453, 2011.

[9] A. C. Gurbuz, J. H. McClellan, and V. Cevher, "A compressive beamforming method," in 2008 IEEE International Conference on Acoustics, Speech and Signal Processing, March 2008, pp. 2617–2620.

[10] P.E. Berry, S. Kodituwakku and K. Venkataraman, ″Generalised phase monopulse for multi-target DoA estimation and extended target spatial imaging″, 2017, Int. Conference on Radar Systems, Belfast, U.K.

[11] P.E. Berry and S. Kodituwakku, ″Real aperture imaging using sparse optimisation with application to low-angle tracking″, 2018 International Conference on Radar, Adelaide, Australia.

[12] B. Ng, L. Rosenberg, and P.E. Berry, "Comparison of Sparse Signal Separation Algorithms for Maritime Radar Target Detection." 2018 International Conference on Radar, Brisbane, Australia.

[13] G. Morris and L. Harkness, Airborne Pulse Doppler Radar, 2dn edition, 1996, Artech House, USA, p307.

[14] B.R. Mahafza, Radar Systems Analysis and Design Using Matlab, Taylor & Francis, 2005, p480.

[15] B.D. Rao and K.V.S. Hari, "Performance analysis of root-music," 22nd Asilomar Conference on Signals, Systems and Computers, Oct 1988, vol. 2, pp. 578–582.

[16] R. Roy and T. Kailath, "ESPRIT-Estimation of Signal Parameters Via Rotational Invariance Techniques", IEEE Trans. Acoustic Speech, vol. 37, No. 7, 1989.

[17] R. Kalman, "A new approach to linear filtering and prediction problems" Transaction of the ASME - Journal of Basic Engineering, vol. 82, no. 1, pp. 35–45, 1960.

[18] Blackman and R. Popoli, Design and Analysis of Modern Tracking Systems, Artech House Norwood, MA, 1999.